Phys Chem Minerals (2008) 35:201–206
DOI 10.1007/s00269-007-0213-3

ORIGINAL PAPER

Magnetic properties and neutron diffraction study of two manganese sulfosalts: monoclinic $MnSb_2S_4$ and benavidesite ($MnPb_4Sb_6S_{14}$)

Philippe Léone · Charlotte Doussier-Brochard · Gilles André · Yves Moëlo

Received: 22 August 2007 / Accepted: 8 December 2007 / Published online: 4 January 2008

Abstract $Mn^{2+}Sb_2S_4$, a monoclinic dimorph of clerite, and benavidesite ($Mn^{2+}Pb_4Sb_6S_{14}$) show well-individualized single chains of manganese atoms in octahedral coordination. Their magnetic structures are presented and compared with those of iron derivatives, berthierite ($Fe^{2+}Sb_2S_4$) and jamesonite ($Fe^{2+}Pb_4Sb_6S_{14}$). Within chains, interactions are antiferromagnetic. Like berthierite, $MnSb_2S_4$ shows a spiral magnetic structure with an incommensurate 1D propagation vector [0, 0.369, 0], unchanged with temperature. In berthierite, the interactions between identical chains are antiferromagnetic, whereas in $MnSb_2S_4$ interactions between chains are ferromagnetic along *c*-axis. Below 6 K, jamesonite and benavidesite have commensurate magnetic structures with the same propagation vector [0.5, 0, 0]: jamesonite is a canted ferromagnet and iron magnetic moments are mainly oriented along the *a*-axis, whereas for benavidesite, no angle of canting is detected, and manganese magnetic moments are oriented along *b*-axis. Below 30 K, for both compounds, one-dimensional magnetic ordering or correlations are visible in the neutron diagrams and persist down to 1.4 K.

P. Léone (✉) · C. Doussier-Brochard · Y. Moëlo
Institut des Matériaux Jean Rouxel,
UMR 6502 CNRS-Université de Nantes,
2 rue de la Houssinière, BP 32229,
44322 Nantes Cedex 03, France
e-mail: Philippe.Leone@cnrs-imn.fr

G. André
Laboratoire Léon Brillouin, CEA-CNRS,
CEA-Saclay, 91191 Gif-s-Yvette Cedex, France

Keywords Manganese · Sulfosalt · Benavidesite · Magnetic properties · Neutron diffraction · Magnetic structure

Introduction

Iron complex minerals of the sulfosalt type, showing well-individualized single chains of iron atoms in octahedral coordination, have been studied previously for their magnetic properties. Magnetic structures of berthierite ($Fe^{2+}Sb_2S_4$) (Winterberger et al. 1990) and jamesonite ($Fe^{2+}Pb_4Sb_6S_{14}$) (Léone et al. 2004) have been thus determined. In this paper, we compare these results with the magnetic structures obtained for manganese derivative compounds, monoclinic $Mn^{2+}Sb_2S_4$, a dimorph of clerite (orthorhombic, isotypic with berthierite) and benavidesite, $Mn^{2+}Pb_4Sb_6S_{14}$ (isotypic with jamesonite).

$MnSb_2S_4$ has been synthesized by solid-state reaction of MnS and Sb_2S_3 following Pfitzner et al. (2000). It crystallizes in the monoclinic symmetry, space group *C2/m*, with unit cell parameters $a = 12.743(3)$, $b = 3.799(1)$, $c = 15.106(3)$ Å and $\beta = 113.91(3)$, $Z = 4$. It is not isotypic with berthierite ($FeSb_2S_4$), which crystallizes in the orthorhombic symmetry, space group *Pnma*, with unit cell parameters $a = 11.412(2)$, $b = 3.763(1)$, $c = 14.161(3)$ Å, $Z = 4$, but it contains the same type of chains of edge-sharing octahedra [MnS_6] parallel to *b*-axis, 6.65 Å apart (Fig. 1).

Benavidesite ($MnPb_4Sb_6S_{14}$) has been synthesized by solid-state reaction of MnS, PbS and Sb_2S_3 (Léone et al. 2003). It crystallizes in the monoclinic symmetry, space group $P2_1/c$, with unit cell parameters $a = 4.0216(8)$, $b = 19.178(4)$, $c = 15.837(3)$ Å and $\beta = 91.89(3)$, $Z = 2$. It is isotopic with jamesonite ($FePb_4Sb_6S_{14}$) (Fig. 2). Mn

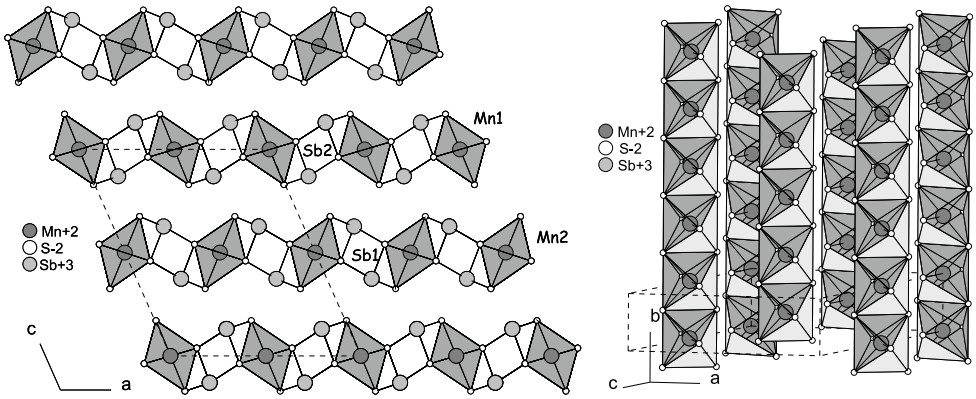

Fig. 1 Crystal structure of monoclinic $MnSb_2S_4$ (*left*), chains of manganese atoms in octahedral coordination (*right*)

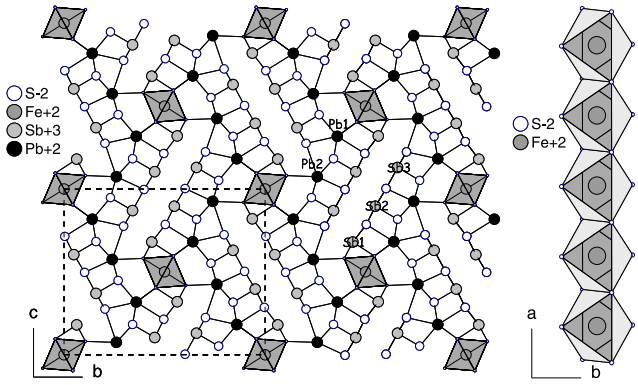

Fig. 2 Crystal structure of jamesonite (benavidesite), $Fe(Mn)Pb_4Sb_6S_{14}$ (*left*); chains of iron (manganese) atoms in octahedral coordination (*right*)

octahedra form single chains parallel to *a*-axis, 12.4 Å apart.

Experimental

Magnetic measurements were carried out on a Quantum Design SQUID magnetometer using powder. The data were corrected for the sample holder contribution and the core diamagnetism using the Pascal's constants.

Calorimetric measurements were performed on a home-made specific heat setup using semi-adiabatic method. Data recorded on sintered pellets were corrected for the sample holder and grease contributions.

The neutron diffraction experiments were performed at the Laboratoire Léon Brillouin (CEA-CNRS) in Saclay (France) using the G4.1 diffractometer ($\lambda = 2.4266$ Å). Height diagrams were collected in the 2θ range 7–86.9° between 1.5 and 160 K (1.5, 5, 10, 15, 20, 25, 40, 160 K) for $MnSb_2S_4$; the data were collected during 3 h at 1.5 K and during 1.5 h at the other temperatures. Sixteen diagrams were collected in the 2θ range 7–86.9° between 1.6 and 45 K (1.6, 3, 4, 5, 6, 7, 10, 13, 16, 18, 21, 24, 27, 30, 34, 45 K) for benavidesite; the data were collected during 5 h at 1.6 K and during 2.5 h at the other temperatures. The samples were set in a cylindrical vanadium can and held in a liquid helium cryostat. Nuclear and magnetic structures were refined using the Rietveld-type (Rietveld 1969) Fullprof (Rodriguez-Carvajal 1990) program. The nuclear scattering lengths and iron magnetic form factor were those included in this program.

Results

Magnetic measurements and specific heat of monoclinic $MnSb_2S_4$

Figure 3 shows the thermal variation of both susceptibility and reciprocal susceptibility of powder under a magnetic field of 1 kOe. At high temperature (above 150 K), the reciprocal susceptibility agrees with a Curie–Weiss law. The effective magnetic moment $\mu_{eff} = 5.9(1)\ \mu_B$ is close to the expected value for high spin Mn^{2+} (5.8–6.0) (Carlin 1986). The Curie paramagnetic temperature $\theta = -63(1)$ K indicates prevalent antiferromagnetic interactions. The susceptibility curve shows a maximum at 25(1) K, corresponding to an antiferromagnetic transition. These results confirm those of Kurowski (2003) ($\theta = -66(1)°$, $T_N = 26.5(5)$ K) except for the effective magnetic moment given by this author, which seems too high ($\mu_{eff} = 6.86(5)\ \mu_B$).

Figure 4 represents the evolution of the susceptibility and of the specific heat versus temperature. The specific heat curve shows a long-range magnetic ordering transition at 23 K corresponding to the antiferromagnetic transition observed on the susceptibility curve, and an additional small peak at 25 K.

The difference between the zero field cooled and the field-cooled data for a field applied of 100 Oe, below 50 K, is illustrated in Fig. 5. The magnetization curves versus applied field recorded at different temperatures are linear above 25 K, showing that the transition temperature has been reached.

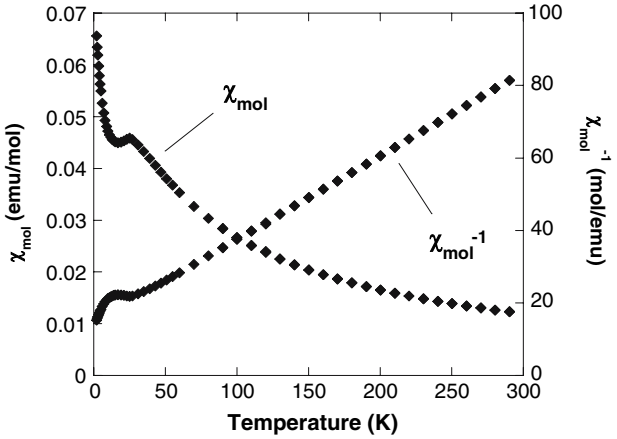

Fig. 3 Temperature dependence of the susceptibility of monoclinic $MnSb_2S_4$ (H = 1 kOe)

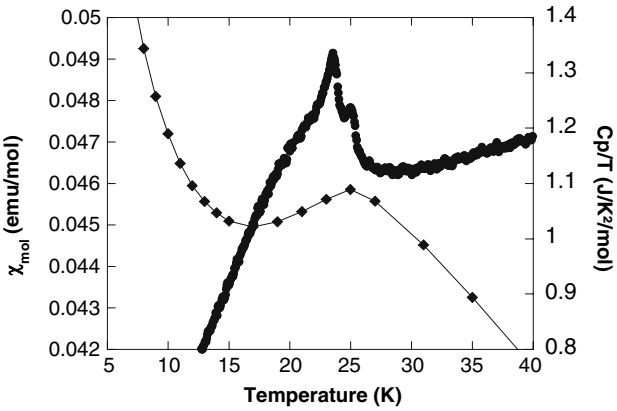

Fig. 4 Observation of the magnetic transition by susceptibility and specific heat measurements of $MnSb_2S_4$

Magnetic structure of monoclinic $MnSb_2S_4$

Figure 6 shows neutron diffraction patterns collected at 1.5, 25 and 160 K. The neutron diffraction pattern recorded at 160 K is strictly due to the nuclear scattering. The sample contains some Sb_2S_3 and MnS as main impurities. The pattern recorded at 25 K evidences the (111) magnetic peak of MnS. Additional peaks of magnetic origin appear below 25 K. Magnetic peaks observed at 1.5 K correspond to a 3D long-range magnetic ordering of manganese magnetic moments. They can be indexed from the nuclear cell parameters using an incommensurate 1D propagation wave-vector along b-axis, equal to $k = [0, 0.369(1), 0]$. Two modulation models were tested, sinusoidal and helicoidal. The best refinement is obtained for the helicoidal model ($R_{mag} = 0.093$). Figure 7 shows observed, calculated and difference neutron diffraction patterns. Figure 8 represents the magnetic structure at 1.5 K. Manganese magnetic moments are oriented in the (a, c) plane. Along the chains of edge-sharing octahedra [MnS_6] (along b-axis), there is an angle of 133° between adjacent magnetic moments; along the a-axis, the angle is 66.85° and it is zero along c-axis. The magnetic moment reaches 4.43(6) μ_B at 1.5 K. The evolution of the magnetic moment values versus temperature is represented in Fig. 9. It confirms the magnetic transition at 25 K. It is remarkable that the propagation vector is unchanged, to the precision of measurements, from 1.5 to 20 K. In his thesis, Kurowski (2003) chose a sinusoidal model for the magnetic structure of $MnSb_2S_4$ ($k_y = 0.371(1)$; M = 4.6(1) μ_B) but later, he and co-authors (Matar et al. 2005; Kurowski et al. unpublished) indicated that the structure is helicoidal, without any detail.

Magnetic measurements and specific heat of benavidesite ($MnPb_4Sb_6S_{14}$)

Previously (Léone et al. 2003), we showed that benavidesite ($MnPb_4Sb_6S_{14}$) has an effective magnetic moment $\mu_{eff} = 5.7(1)$ μ_B and a Curie paramagnetic temperature $\theta = -40$ K, characteristic of high spin Mn^{2+} with antiferromagnetic interactions (Fig. 10). The evolution of the specific heat versus temperature (Fig. 11) and the zero field cooled (ZFC), field cooled (FC) susceptibility curves for an applied field of 100 Oe (Fig. 12) show a long-range magnetic ordering transition at about 6 K. Between 6 and 45 K, ZFC and FC susceptibility curves do not coincide: this difference may be attributed to 1D magnetic ordering, or to

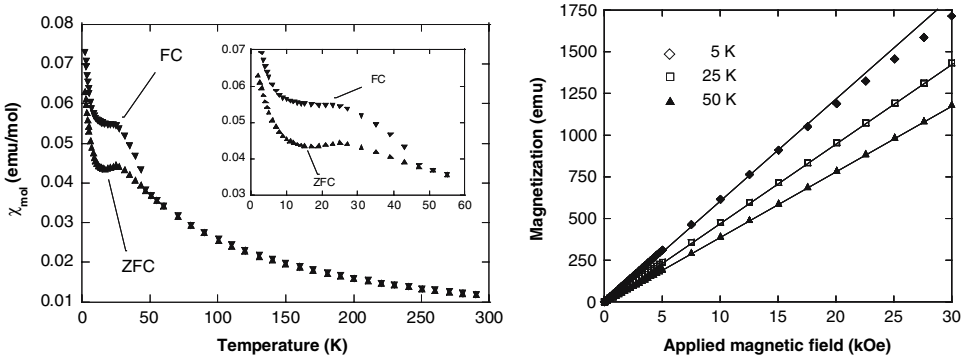

Fig. 5 Susceptibility of $MnSb_2S_4$ (H = 100 Oe): field cooled (FC) and zero field cooled (ZFC) (*left*), magnetization versus applied magnetic field (*right*)

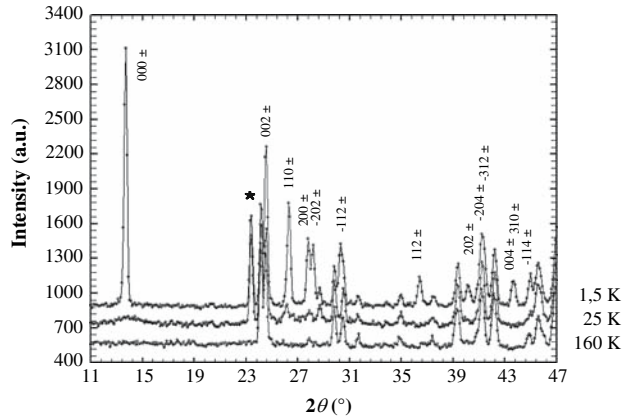

Fig. 6 Part of neutron diffraction patterns of monoclinic $MnSb_2S_4$ at 1.5, 25 and 160 K; at 1.5 and 25 K, the peak marked with an *asterisk* is the (111) magnetic peak of MnS

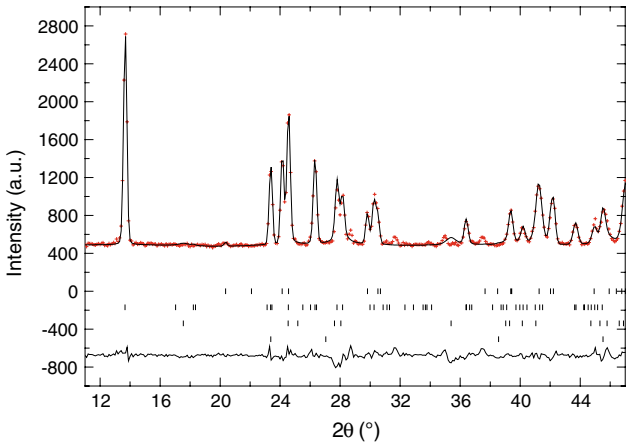

Fig. 7 Observed (*cross*), calculated (*solid line*) and difference (*solid line at the bottom*) neutron diffraction patterns at 1.5 K of $MnSb_2S_4$. The first series (*up*) of Bragg reflexion markers corresponds to the nuclear structure, the second series to the magnetic structure, the third series to Sb_2S_3 and the fourth (*down*) to MnS

correlations along the manganese octahedra which form single chains in the structure. The magnetization curves versus applied field recorded are linear at 5 K.

Magnetic structure of benavidesite ($MnPb_4Sb_6S_{14}$)

Figure 13 shows neutron diffraction patterns collected at 1.6, 6 and 45 K. The neutron diffraction pattern recorded at 45 K is strictly due to the nuclear scattering. The sample contains one Mn-free impurity, robinsonite ($Pb_4Sb_6S_{13}$). A series of extra peaks is present at 1.6 K corresponding to the three-dimensional long-range magnetic ordering of the manganese magnetic moments. These magnetic peaks can be indexed in doubling the *a* parameter of the crystal cell. These extra peaks have disappeared at 6 K. Like jamesonite ($FePb_4Sb_6S_{14}$) (Léone et al. 2004), at around $2\theta = 18°$, the background of all neutron diagrams exhibits a step which disappears at around 30 K. In order to determine the magnetic structure, to limit the number of parameters, we used the results of the group theory calculation. Contrary to jamesonite, the best fit (Fig. 14) is obtained for the "Γ_4" irreductible representation and not for "Γ_2". Despite the results of the group theory calculation define the moment vector by three parameters, the magnetic moments are strictly oriented along *b*-axis (Fig. 15) and reach 3.2(1) μ_B at 1.6 K. The magnetic reliability factor ($R_{mag} = 0.159$) is a little bit high ($R_{mag} = 0.126$ for jamesonite): two possible explanations are the weak intensity of the magnetic peaks compared to nuclear one, as well as the small amount of sample.

Discussion

Comparison between berthierite ($FeSb_2S_4$) and monoclinic $MnSb_2S_4$

Within single chains of Fe or Mn octahedra, according to Goodenough-Kanamori rules (Goodenough 1963), super-exchange interactions at 90° are antiferromagnetic. In berthierite ($FeSb_2S_4$) (Winterberger et al. 1990), the distances between neighbouring chains are smaller (6.19 Å) than those in $MnSb_2S_4$ (6.65 Å), and the interactions are stronger, leading to a 3D long-range magnetic ordering at higher

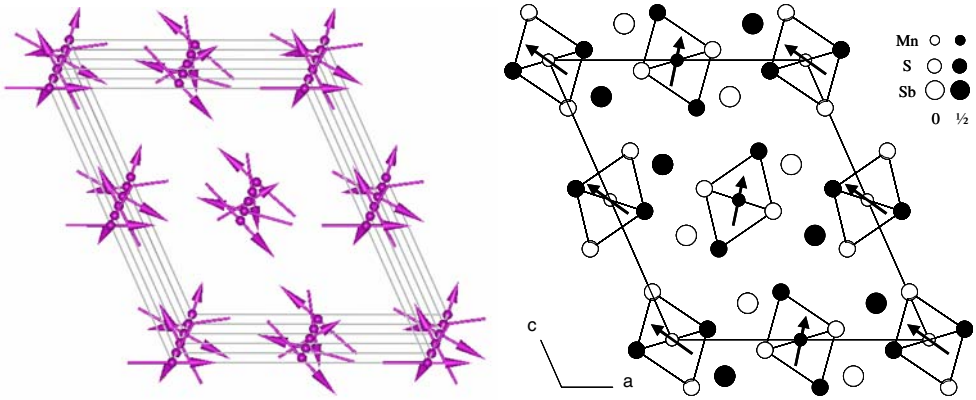

Fig. 8 $MnSb_2S_4$ magnetic structure: drawing in perspective (*left*), in projection along the *b*-axis (*right*)

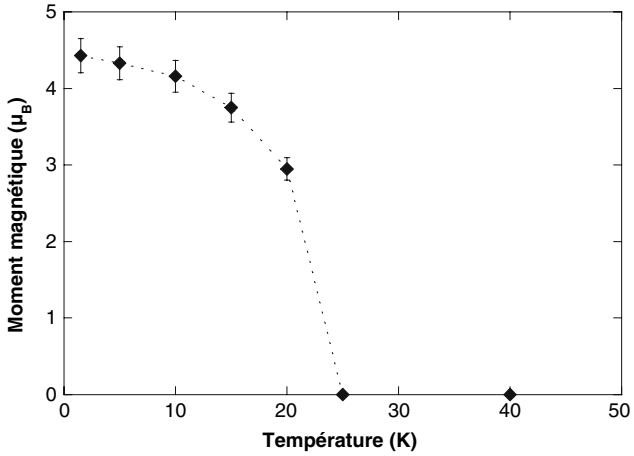

Fig. 9 Evolution of the magnetic moment versus temperature for monoclinic $MnSb_2S_4$

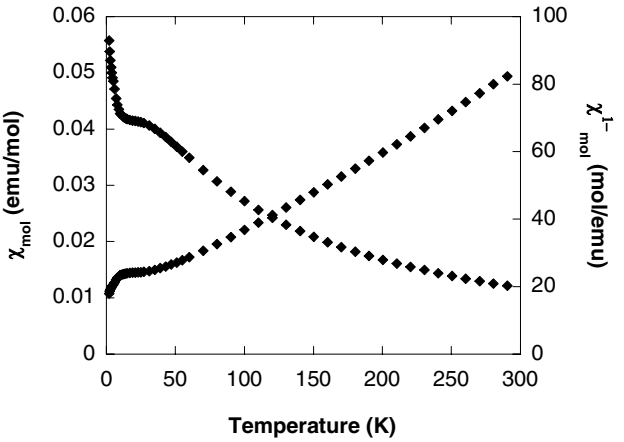

Fig. 10 Temperature dependence of the susceptibility of benavidesite ($MnPb_4Sb_6S_{14}$) (H = 1 kOe)

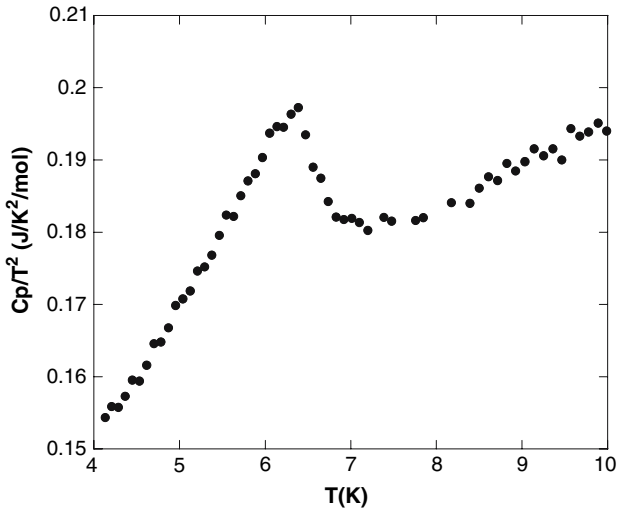

Fig. 11 Observation of the magnetic transition by specific heat measurements of benavidesite

temperature, 50 K instead of 25 K. Both compounds show spiral magnetic structures with a similar incommensurate 1D propagation vector (k_y = 0.394 for $FeSb_2S_4$ and 0.369 for $MnSb_2S_4$), unchanged with temperature, and no short range magnetic order is detectable on neutron diagrams just above T_N. In berthierite, the interactions between identical chains (6.19 Å apart) are antiferromagnetic, whereas in $MnSb_2S_4$, interactions between chains along c-axis (Fig.8) (7.55 Å apart) are ferromagnetic. The maximum magnetic moment values, 4.1 μ_B for iron II and 4.4 μ_B for manganese II, are close to expected ones, respectively 4 and 5 μ_B.

Comparison between jamesonite ($FePb_4Sb_6S_{14}$) and benavidesite ($MnPb_4Sb_6S_{14}$)

The ZFC-FC susceptibility measurements, the evolution of the specific heat and the powder neutron diffraction patterns of benavidesite ($MnPb_4Sb_6S_{14}$) show, like for jamesonite ($FePb_4Sb_6S_{14}$) (Léone et al. 2004), a 3D long-range magnetic ordering at 6 K. Jamesonite is a canted ferromagnet and iron magnetic moments are mainly oriented along a-axis. On the contrary, no angle of canting is detected for benavidesite, and manganese magnetic moments are oriented along b-axis.

For both compounds, we observed an increase on the background in the neutron diffraction pattern at about $2\theta = 17°$, below 30 K. This "step" can be most probably attributed to 1D magnetic ordering, or correlations along the iron or manganese octahedra which form single chains in the structure: the distance between iron or manganese atoms along these chains is equal to the a parameter (4.02 Å), so $Q = \pi/a = 0.78$ Å^{-1} and it corresponds to $2\theta = 17.5$ [=2 arcsin($Q\lambda/4\pi$)]. Below 6 K, a few chains remain uncorrelated giving rise to this 1D magnetic signal. Probably, it explains the smaller maximum magnetic moment value, 3.3 μ_B for iron II and 3.2 μ_B for manganese II, than expected, respectively 4 μ_B and 5 μ_B. Morimoto et al. (2007), by Mössbauer spectroscopy of a synthetic jamesonite sample, did not detect any development of this short-range magnetic order. They explain the Mössbauer spectra by the development of a spin-glass state and a 3D magnetic order.

Comparison between (berthierite, monoclinic $MnSb_2S_4$) and (jamesonite, benavidesite)

All these compounds present crystal structures with 1D organization in which iron or manganese octahedra form single chains. In jamesonite and benavidesite, the distances between neighbouring chains are larger (12.3 Å) than in berthierite and monoclinic $MnSb_2S_4$, so the interactions are weaker, leading to a 3D long-range ordering at lower temperature (6 K), a commensurate magnetic structure, and a

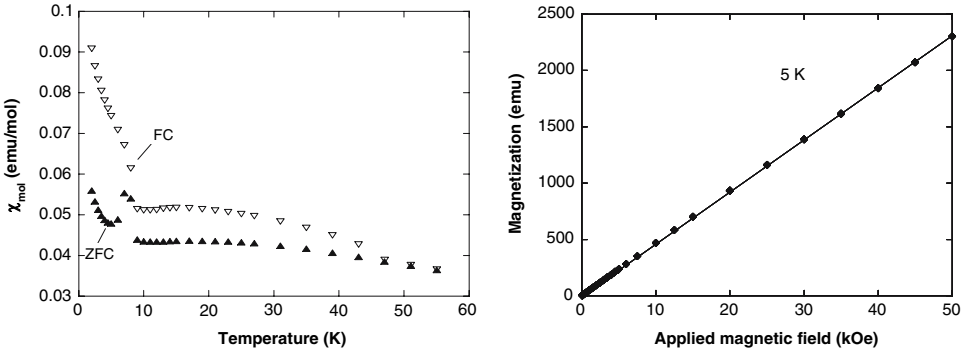

Fig. 12 Susceptibility of benavidesite (H = 100 Oe): field cooled (FC) and zero field cooled (ZFC) (*left*), magnetization versus applied magnetic field (*right*)

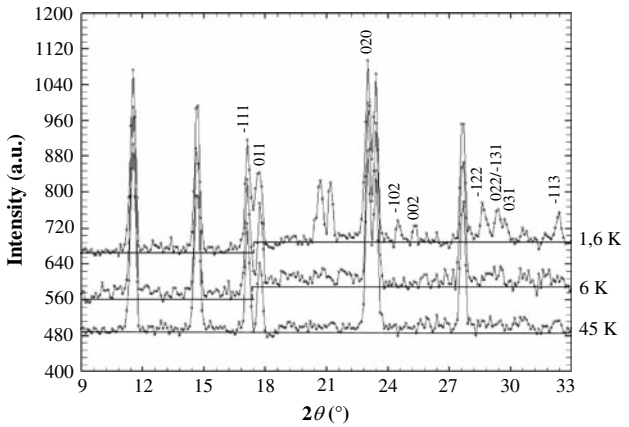

Fig. 13 Part of neutron diffraction patterns of benavidesite ($MnPb_4Sb_6S_{14}$) at 1.6, 6 and 45 K. Relatively to the diagram at 45 K, those at 6 and 1.6 K have been shifted up for clarity. For each temperature, a line is drawn to show the evolution of the background

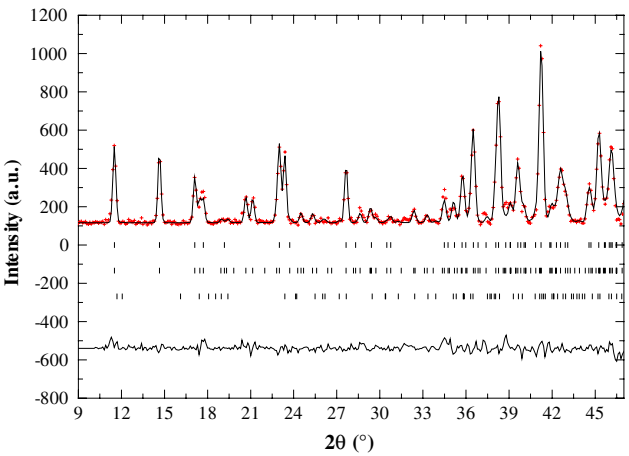

Fig. 14 Observed (*cross*), calculated (*solid line*) and difference (*solid line at the bottom*) neutron diffraction patterns at 1.6 K of benavidesite. The first series of Bragg reflexion markers corresponds to the nuclear structure, the second series to the magnetic structure, the third series to robinsonite ($Pb_4Sb_6S_{13}$)

1D magnetic correlations below 30 K. For berthierite and $MnSb_2S_4$, the interactions between chains lead to a spiral magnetic structure and no short-range order is detectable.

Fig. 15 Benavidesite ($MnPb_4Sb_6S_{14}$) magnetic structure

Acknowledgments We thank Dr. P. Molinié and Dr. E. Janod (Institut des Matériaux Jean Rouxel, Nantes) for their help in magnetic and calorimetric measurements, as well as for fruitful discussions.

References

Carlin RL (1986) Magnetochemistry. Springer, Heidelberg

Goodenough JB (1963) Magnetim and chemical bond. Wiley Intersciences, London

Kurowski D (2003) Mangan-Chalkogenometallate der 15. Gruppe und binäre Kupfertelluride. Ph.D. thesis. University of Regensburg, Regensburg

Léone P, Le Leuch L-M, Palvadeau P, Molinié P, Moëlo Y (2003) Single crystal structures and magnetic properties of two iron or manganese-lead-antimony sulfides: $MPb_4Sb_6S_{14}$ (M: Fe,Mn). Solid State Sci 5:771–776

Léone P, André G, Doussier C, Moëlo Y (2004) Neutron diffraction study of the magnetic ordering of jamesonite ($FePb_4Sb_6S_{14}$). J Magn Magn Mater 284:92–96

Matar SF, Weihrich R, Kurowski D, Pfitzner A, Eyert V (2005) Electronic structure of the antiferromagnetic semiconductor $MnSb_2S_4$. Phys Rev B 71:235207-1–235207-9

Morimoto S, Matsushita Y, Ueda Y, Kawase M, Saito T, Nakamura S, Nazu S (2007) ^{57}Fe Mössbauer spectroscopy of pseudo-1D sulfide of $FePb_4Sb_6S_{14}$. J Magn Magn Mater 310:e962–e964

Pfitzner A, Kurowski D (2000) A new modification of $MnSb_2S_4$ crystallizing in the $HgBi_2S_4$ structure type. Z Kristallogr 2:373–376

Rietveld HM (1969) A profile refinement method for nuclear and magnetic structures. J Appl Cryst 2:65–71

Rodriguez-Carvajal J (1990) A program for Rietveld refinement and pattern matching analysis. Abstracts of the satellite meeting on powder diffraction of the XV congress of the IUCr:127

Winterberger M, André G (1990) Magnetic properties and spiral magnetic structure of berthierite $FeSb_2S_4$. Physica B 162:5–12